Journal of the European Ceramic Society 18 (1998) 565–582

PII: S0955-2219(97)00151-9
0955-2219/98/$19.00 + 0.00

Preparation of Oxalate Precursor of PLZT. Characterization of the Individual Components

M. Pereira and P. Q. Mantas

Departamento de Engenharia Cerâmica e do Vidro, Universidade de Aveiro 3810 Aveiro, Portugal

(Received 18 April 1997; accepted 11 August 1997)

Abstract

The stability behaviour of each individual component of PLZT, in aqueous solutions of oxalic acid, has been investigated. The aim of this study was, on the one hand, to better understand the chemistry of the different metal ions in complexation with $C_2O_4^{2-}$ and OH^-, and in the other hand, to define the effect of pH on the structure of the precipitate and in its formation yield stability calculations for the different soluble metal complexes were firstly done starting from the available constants. Then, for each ion, a convenient pH and concentration range has been established for quantitative precipitation. By application of the calculations, metallic salts were precipitated from solutions containing aqueous oxalic acid and ammonia. Some unexpected and unknown precipitates have been synthesized. These new crystalline phases have been identified by different techniques (TGA, FTIR, XRD). © *1998 Elsevier Science Limited. All rights reserved*

1 Introduction

Ceramics based on he perovskite structure ABO_3, where A^{n+} (Ba^{2+}, Pb^{2+}, ...) forms cubically close packed layers with O^{2-}, while B^{m+} (Ti^{4+}, Zr^{4+}, Ta^{5+}, Nb^{5+}...) occupy the octahedral interstices surrounded by O^{2-}, have been intensively studied because of their spontaneous polarization.[1] Among them, lead titanate zirconate (PZT) ceramics are known to present pronounced piezoelectric-ferroelectric behavior and high Curie point. In this family, La modified PZT can be obtained by partial substitution of Pb^{2+} by La^{3+}. The main property of these materials is the combination of good optical transparency with strong electro-optic effects and ferroelectric switching. These characteristics depend on the La content, the Zr/Ti ratio,[3] and on the microstructure of the sintered material. PLZT materials, which are to be considered for optical applications, should have high density, controlled microstructure and grain size, and chemical homogeneity.

PLZT ceramics were firstly obtained by classical solid state reactions of mechanically mixed oxides (MO–PLZT) sintered at high temperatures (> 1000°C). However, the volatility of PbO at high temperature induces compositional variations, residual porosity and grain growth, limiting the electro-optical properties.[4–7] In order to avoid these phenomena, chemical preparation of powders via precursor decomposition has been extensively investigated: for these new powders, the homogeneity of composition is controlled at the atomic scale, and owing to their nanosized grain, the sinterability at low temperature is improved. Moreover, the use of a precursor allows the elaboration of high purity powders since it is directly correlated with the initial reagents, and the experimental conditions.[8] Among the primary reagents, the metal-alkoxides have been used by solution-decomposition method, either alone,[9–11] or mixed with metal oxide powders.[12,13] Unfortunately, these organometallic precursors are expensive, and must be handled carefully because of their high sensitivity to moisture, heat and light. For these restrictive reasons, a high scale production is out of order.

The use of mineral salts as starting reagents, like nitrates or chlorides, leads to a relatively inexpensive process. Aqueous solutions of the four different salts are mixed. A coprecipitation agent is then added to produce the cation mixed precipitate. The synthesis of metal carbonates,[14] hydroxides,[15–17] citrates...[18] precursors has been extensively reported.

In the present work, we chose the oxalic acid as the complexing agent for PLZT, since it has been successfully used for the synthesis of $BaTiO_3$, $PbTiO_3$ and $Pb_xBa_{1-x}TiO_3$ powders.[19–21] But, the

more the number of metal ions, the more difficult is the chemical process to carry out. Some authors have already reported the preparation of PLZT by this method. Yamamura *et al.*,[22] starting from nitrates of Pb and La and oxynitrates of Zr and Ti, obtained the precipitate by oxalate titration. The precipitation was done in ethanol solution. at 30°C, but part of the metallic cations did not pass into the mixed oxalate. Moreover, the resulting precursor needed to reach 800–900°C to decompose into a single phase of the perovskite type structure. In order to increase the coprecipitation yield, Song *et al.*,[23] reported a modification to Yamamura's process by raising the pH of the solution. The precipitate formed was also calcined at high temperature (1000°C), but the composition of the final powder was correctly controlled.

The aim of the present study is to develop a low cost aqueous process allowing to obtain (i) high purity and reactivity fine powder after low temperature calcination, (ii) good chemical homogeneity and composition control from the mixing salts step to the final sintered ceramic. and (iii) fair densification, without the use of the hot pressing or sintering aids, leading to a ceramic with good optical and electrical properties. In this first part, we check the characteristics of stability and precipitation of the different metallic individual components, in order to better understand the precipitation in an aqueous solution of the mixed-cation oxalate. In the second part, we'll see the precipitation of the mixed ion oxalate and its decomposition in order to get pure PLZT perovskite phase.

The different elaboration processes presented above were based on empirical results, leading to an improvement of the experimental conditions step by step. The calculation of the stability conditions for various concentrations of ligands and of metals can help to find explanations to empirical experiments and also to define optimum parameters to obtain high yield of precipitation. Very few authors[24,25] have attempted to examine the behaviour of the different ions in an aqueous solution, on a theoretical basis. The main difficulty to do that is the lack of chemical stability data for most of the complexes. Some compilations[26–28] of stability constants are available, but sometimes the experimental conditions (as ionic strength, temperature...) are not indicated. Also, wide variations often found for metal complex constants are originated by different sources such as impure ligands, poor experimental design, faulty experimental conditions, or inaccurate measurements.[29] If well-established data are available, then the present approach should be sufficiently accurate to allow qualitative and quantitative analysis of the calculated results.

2 Theoretical Approach

When we want to prepare powder precursors from a precipitation process, we normally mix solutions containing the desired ions with a complexing agent in order to get a precipitate. In many cases, this procedure leads to the formation of the desired precipitate, but with low yield, or to the formation of undesired precipitates, because usually the solubility of the different species in solution is not taken into account. In our case, we want to check the behaviour of the individual cations, Pb, La, Zr and Ti, in the presence of oxalic acid in order to get an oxalate precipitate. The concentration of the different components (metal ions, ligands, acid/base) and their chemical nature, will lead to final solutions with different pH values. A variation in the pH value will change either the yield or the type of the obtained precipitate, and so, it is very important to know which is the best pH range to get our precipitate. This can be done empirically, but here, we try to show how theoretical calculations can solve this problem in one step.

In this work, the procedure adopted was the following: (i) firstly, we determined the behaviour of any cation in solution when pH is changed, and (ii) secondly, we checked the changes in this solution behaviour after the addition of the oxalic acid. The first point is enough for the calculations of precipitate formation when one wants to obtain hydroxide precursors; the second one can also be used to obtain other type of precipitate than oxalates. In both cases, the aim of the calculations is: at a fixed pH value, what is the amount of the non-precipitated cations in the solution; if the initial cation concentration in the solution is lower than this value, there is no precipitate formation, while for higher concentrations, the difference is the amount of precipitate obtained. The Appendix shows how this can be done for the hydroxide and/or oxalate formation, either generally or for the cases under study. The main results are in Section 3. In Sections 4 and 5, we compare the previsions of the calculations with experimental results.

3 Application of the Calculations to Each Individual Component

3.1 Stability constants

Table 1 presents the various stability constants taken into account for the calculation. These

Table 1. Stability constants for the Pb^{2+}-La^{3+}-Zr^{4+}-TiO^{2+}-OH^{-}9 $C_2O_4^{2-}$ systems

Equilibrium reactions	*Constants*	*Eqn.*	*Ref.*
$H^+ + C_2O_4^{2-} \Longleftrightarrow HC_2O_4^-$	$\log K_1 = 1{\cdot}22$	(1)	25,26,30
$H^+ + HC_2O_4- \Longleftrightarrow H_2C_2O_4$	$\log K_2 = 3{\cdot}64$	(2)	25,26,30
$Pb^{2+} \Longleftrightarrow Pb(OH)^+ + H^+$	$\log {}^*\beta_1 = -7{\cdot}86$	(3)	25
$Pb^{2+} \Longleftrightarrow Pb(OH)_2{}^0_{aq.} + 2\,H^+$	$\log {}^*\beta_2 = -17{\cdot}26$	(4)	25
$Pb^{2+} \Longleftrightarrow Pb(OH)^{3-} + 3\,H^+$	$\log {}^*\beta_3 = -28$	(5)	25
$2\,Pb^{2+} \Longleftrightarrow Pb_2(OH)^{3+} + H^+$	$\log {}^*\beta_{12} = -6{\cdot}16$	(6)	25
$3\,Pb^{2+} \Longleftrightarrow Pb_3(OH)_4{}^{2+} + 4\,H^+$	$\log {}^*\beta_{43} = -23{\cdot}95$	(7)	25
$4\,Pb^{2+} \Longleftrightarrow Pb_4(OH)_4{}^{4+} + 4\,H^+$	$\log {}^*\beta_{44} = -20{\cdot}30$	(8)	25
$6\,Pb^{2+} \Longleftrightarrow Pb_6(OH)_84^+ + 8\,H^+$	$\log {}^*\beta_{86} = -43{\cdot}3$	(9)	25
$Pb(OH)_{2\ prec.} + 2H^+ \Longleftrightarrow Pb^{2+}$	$\log {}^*K_{so} = 13{\cdot}0$	(10)	25
$Pb^{2+} + C_2O_4^{2-} \Longleftrightarrow Pb(C_2O_4)^0_{aq.}$	$\log \beta_1 = 3{\cdot}50$	(11)	25,26
$Pb^{2+} + 2C_2O_4^{2-} \Longleftrightarrow Pb(C_2O_4)_2{}^{2-}$	$\log \beta_2 = 6{\cdot}50$	(12)	25,26
$Pb(C_2O_4)_{\ prec.} \Longleftrightarrow Pb^{2+} + C_2O_4^{2-}$	$\log K_{so} = -9{\cdot}3$	(13)	30
$La^{3+} \Longleftrightarrow La(OH)^{2+} + H^+$	$\log {}^*\beta_1 = -8{\cdot}5$	(14)	28
$La^{3+} \Longleftrightarrow La(OH)^{2+} + 2H^+$	$\log {}^*\beta_2 = -17{\cdot}2$	(15)	28
$La^{3+} \Longleftrightarrow La(OH)_3{}^0_{aq.} + 3H^+$	$\log {}^*\beta_3 = -25{\cdot}9$	(16)	28
$La^{3+} \Longleftrightarrow La(OH)_4^- + 4H^+$	$\log {}^*\beta_4 = -36{\cdot}9$	(17)	28
$2\,La^{3+} \Longleftrightarrow La_2(OH)^{5+} + H^+$	$\log {}^*\beta_{12} = -9{\cdot}98$	(18)	26
$5\,La^{3+} \Longleftrightarrow La_5(OH)_9{}^{6+} + 9H^+$	$\log {}^*\beta_{95} = -71.2$	(19)	26
$La(OH)_{3\ prec.} + 3H^+ \Longleftrightarrow La^{3+}$	$\log {}^*K_{so} = 19{\cdot}7$	(20)	28
$La^{3+} + C_2O_4^{2-} \Longleftrightarrow La(C_2O_4)^+$	$\log \beta_1 = 4.3$	(21)	26
$La^{3+} + 2C_2O_4^{2-} \Longleftrightarrow (La(C_2O_4)_2^-$	$\log \beta 2 = 7{\cdot}9$	(22)	26
$La^{3+} + 3C_2O_4^{2-} \Longleftrightarrow (La(C_2O_4)_3{}^0_{aq.}$	$\log \beta_3 = 10{\cdot}3$	(23)	26
$La_2(C_2O_4)_{3\ prec.} \Longleftrightarrow 2La^{3+} + 3C_2O_4{}^{2-}$	$\log K_{so} = -25$	(24)	26
$Zr^{4+} \Longleftrightarrow Zr(OH)^{3+} + H^+$	$\log {}^*\beta_1 = -0{\cdot}6$	(25)	25
$Zr^{4+} \Longleftrightarrow Zr(OH)_2{}^{2+} + 2H^+$	$\log {}^*\beta_2 = -2{\cdot}1$	(26)	25
$Zr^{4+} \Longleftrightarrow Zr(OH)_3{}^+ + 3H^+$	$\log {}^*\beta_3 = -6{\cdot}5$	(27)	25
$Zr^{4+} \Longleftrightarrow Zr(OH)_4{}^0_{aq.} + 4H^+$	$\log {}^*\beta_4 = -11{\cdot}2$	(28)	25
$Zr^{4+} \Longleftrightarrow Zr(OH)_5^- + 5H^+$	$\log {}^*\beta_5 = -17$	(29)	25
$3\,Zr^{4+} \Longleftrightarrow Zr_3(OH)_4{}^{8+} + 4H^+$	$\log {}^*\beta_{43} = 5{\cdot}1$	(30)	25
$3\,Zr^{4+} \Longleftrightarrow Zr_3(OH)_5{}^{7+} + 5H^+$	$\log {}^*\beta_{53} = 5{\cdot}5$	(31)	25
$4\,Zr^{4+} \Longleftrightarrow Zr_4(OH)_8{}^{8+} + 8H^+$	$\log {}^*\beta_{84} = 8{\cdot}0$	(32)	25
$Zr(OH)_{4\ prec.} + 4H^+ \Longleftrightarrow Zr^{4+}$	$\log {}^*K_{so} = -0{\cdot}4$	(33)	25
$Zr^{4+} + C_2O_4^{2-} \Longleftrightarrow (Zr(C_2O_4)^{2+}$	$\log \beta_1 = 10{\cdot}40$	(34)	25,26
$Zr^{4+} + 2\,C_2O_4^{2-} \Longleftrightarrow (Zr(C_2O_4)_2{}^0$	$\log \beta_2 = 19{\cdot}40$	(35)	25,26
$TiO^{2+} \Longleftrightarrow TiO(OH)^+ + H^+$	$\log {}^*\beta_1 = -2{\cdot}5$	(36)	24,25
$TiO^{2+} \Longleftrightarrow TiO(OH)_2{}^0_{aq.} + 2H^+$	$\log {}^*\beta_2 = -5{\cdot}0$	(37)	24,25
$TiO^{2+} \Longleftrightarrow TiO(OH)_3{}^- + 3\,H^+$	$\log {}^*\beta_4 = 53{\cdot}3$	(38)	27
$8\,TiO^{2+} \Longleftrightarrow TiO_8(OH)_{12}{}^{4+} + 12H^+$	$\log {}^*\beta_{128} = -1{\cdot}68$	(39)	24
$TiO(OH)_{2\ prec.} + 2H^+ \Longleftrightarrow TiO^{2+}$	$\log {}^*K_{so} = -0{\cdot}5$	(40)	25
$TiO^{2+} + C_2O_4^{2-} \Longleftrightarrow (TiO(C_2O_4))^0_{aq.}$	$\log \beta_1 = 6{\cdot}60$	(41)	25
$TiO^{2+} + 2C_2O_4^{2-} \Longleftrightarrow (TiO(C_2O_4)_2{}^{2-}$	$\log \beta_2 = 10{\cdot}70$	(42)	25

values were chosen, when possible, for ionic strength equal to 0·1, at 25°C[24–28,30]. The notation used to describe each equilibrium is the one proposed by the IUPAC.[26] Since some variations were found for several constants, because of the reasons explained before. the stability diagrams should be considered as a relatively good approximation of the real solution.

3.2 Pb^{2+} aqueous solution

3.2.1 Hydroxide precipitation

The result of the calculations applied to the formation of lead hydroxide precipitate is presented in Fig. 1. This diagram exhibits different domains of complex stability. The different straight lines correspond to the concentration of the various complexes that can be found in an aqueous solution of Pb^{2+}, as a function of pH. The solid line corresponds to the limit of solubility of the Pb complexes, and so to the beginning of the precipitation of $Pb(OH)_2$. This line is the direct representation of eqn (A7) as a function of pH.

In common conditions, $[Pb]_0 < 0{\cdot}07$ mol l^{-1}, and taking this value as an example, it can be seen that the precipitation highly depends on the acidity level of the solution. In equilibrium conditions of precipitation, the solid hydroxide phase can be formed

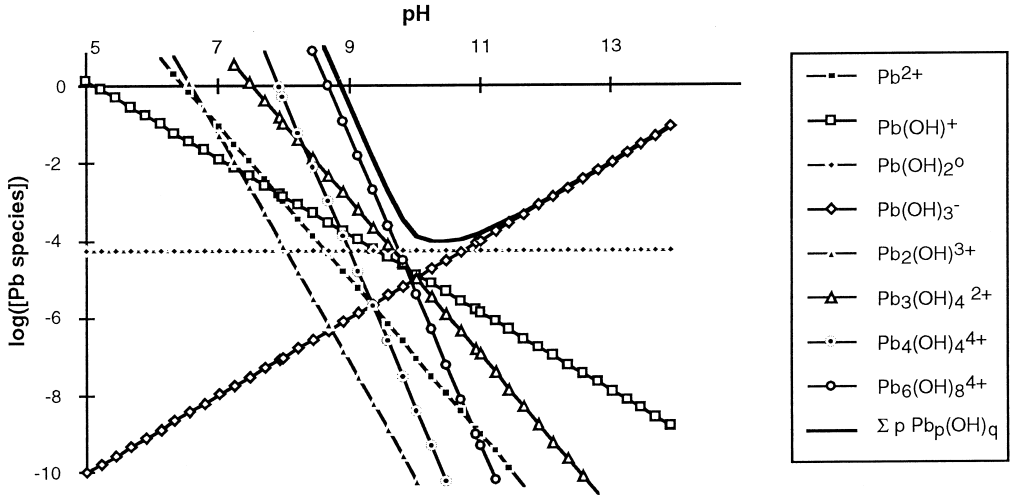

Fig. 1. Stability diagram for complexes formation in the Pb–H_2O system.

when pH reaches 8·9, as expected when basic species OH^- are present. The decrease of the $[Pb]_o$ concentration reduces the pH stability domain for precipitation in such way that, for $[Pb]_0 = 10^{-3}$ mol l^{-1}, the hydroxide precipitate is only stable in the pH range 9·7–11·9. At higher pH, lead ions pass into the solution by the formation of the $Pb(OH)_3^-$ compound. On the other hand, $Pb_6(OH)_8^{4+}$ and $Pb(OH)_2^0$ aq., the major components of the solution for pH < 10·8, are the main species responsible for the low precipitation yield at low pH. The result is that, if one wants a quantitative precipitation of hydroxide from a solution of Pb^{2+}, the initial concentration $[Pb]_0$ must be higher than $10^{-4.03}$ mol l^{-1}, and the pH has to be adjusted as high as 9 (for high concentrated solutions). The Ringbom side-component reaction coefficient was calculated and plotted in Fig. 2; this coefficient exhibits a minimum for the side reaction at pH = 10, i.e. far from this value, mono- and poly-nuclear complexes become the main components of the solution. It is worth noting that the calculation is strongly dependent on the solubility product, for which a small decrease gives an expansion of the precipitate stability area, and also a lower ratio of the side-reaction components.

3.2.2 Oxalate precipitation

By addition of oxalic acid, the hydroxide stability field is reduced by important formation of $Pb(C_2O_4)_i^{(2-2i)}$ ($i = 1, 2$) species. Moreover, oxalic acid increases the formation of soluble species for high pH conditions, thus lowering the precipitation yield. The diagram of Fig. 3. corresponds to the reaction:

$$\left(Pb(OH)_2\right)_{prec.} + 2H^+ + C_2O_4^{2-} \Longleftrightarrow \left(PbC_2O_4\right)_{prec.} + 2H_2O \qquad (1)$$

The curves there represented correspond to the following equations:

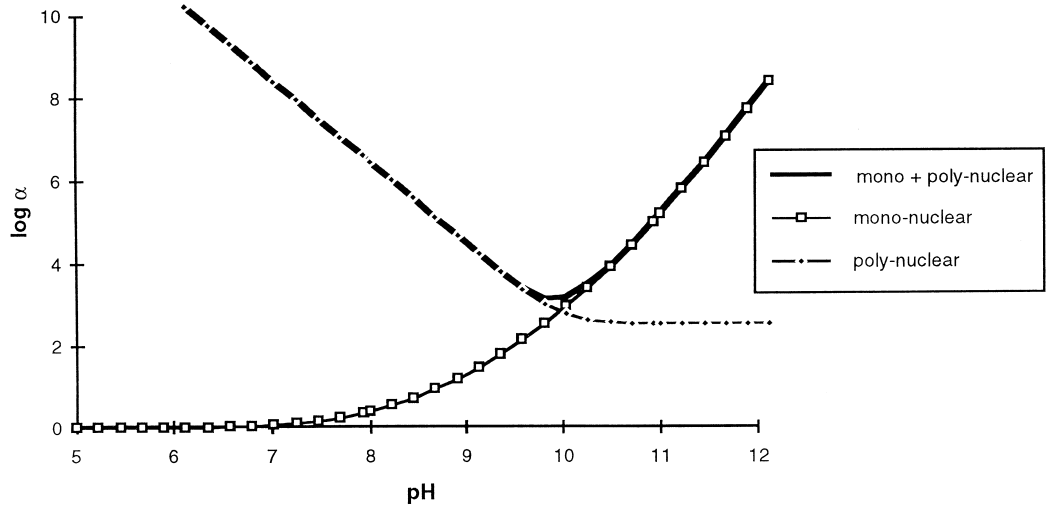

Fig. 2. Evolution of Ringbom's side reaction coefficient for different pH values.

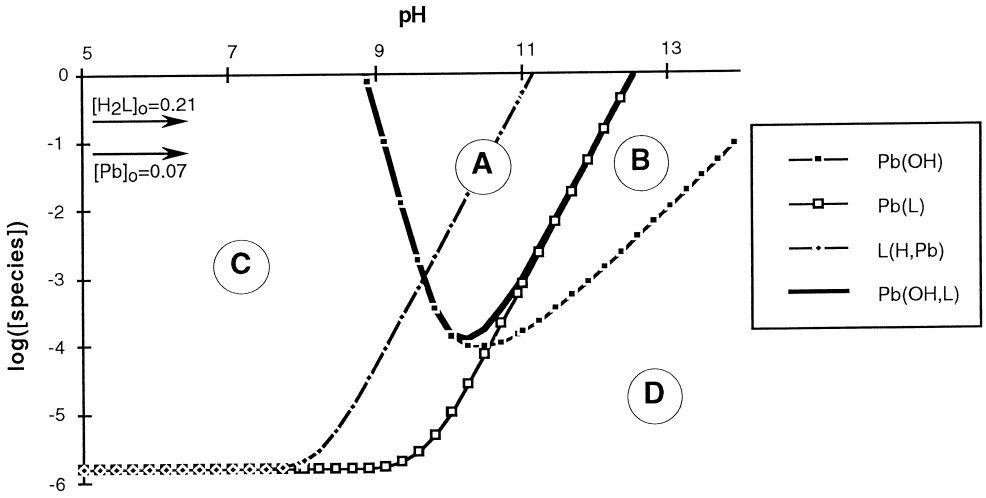

Fig. 3. Stability diagram for complexes formation in the Pb–oxalic acid–H_2O system.

$$\sum \mathrm{Pb[OH]} = \mathrm{Pb} + \mathrm{Pb(OH)} + \mathrm{Pb(OH)_3} + 2\mathrm{Pb_2(OH)} + 3\mathrm{Pb_3(OH)_4} + 4\mathrm{Pb_4(OH)_4} + 6\mathrm{Pb_6(OH)_8} + \left(\mathrm{Pb(OH)_2}\right)_{\mathrm{aq.}} \quad (2)$$

$$\sum \mathrm{Pb[L]} = \mathrm{Pb(L)} + \mathrm{Pb(L)_2} \quad (3)$$

$$\sum \mathrm{Pb[OH,\ L]} = \sum \mathrm{Pb[OH]} + \sum \mathrm{Pb[L]} \quad (4)$$

$$\sum \mathrm{L[H,\ Pb]} = \mathrm{L} + \mathrm{HL} + \mathrm{H_2L} + \mathrm{Pb(L)} + 2\mathrm{Pb(L)_2} \quad (5)$$

It must be noted that eqn (2) is not exactly the sum of the hydroxide species, but it allows to get directly the hydroxide precipitate formation through eqn (A1). Also, only eqns (4) and (5) concern the mass balance.

The large increase of the concentration of oxalic derived species in the solution, curve L(H, Pb) in Fig. 3, starting at pH = 8, is essentially due to the formation of non metal species, since this line is higher than the $\sum$Pb[L] one. Thus, the equilibrium condition for the two precipitates is described in the diagram by the 'parabolic' region (marked A) formed by the Pb(OH, L) curve. In the area of intersection with L(Pb, H) curve, the stability domain of lead oxalate precipitation is defined. The diagram indicates two possible initial concentrations, $[H_2L]_0$ and $[Pb]_0$, values that will be used for the preparation of the PLZT materials. Taking these values as a practical example, the diagram indicates that both are sufficient to allow the formation of the two precipitates simultaneously in a straight range of pH; elsewhere. only one of the precipitates is formed. In the (A) area, the concentration of soluble species is at least 10^{-3} mol l^{-1}, which is 10 times the hydroxide ratio without oxalic acid addition.

3.2.3 Out of dual precipitation equilibrium

In the case where $[Pb]_0 > \sum$Pb[OH], but with insufficient $[H_2L]_0$ (pH > 12·2) in our example), area marked B in Fig. 3, the precipitation of $Pb(OH)_2$ appears with high yield near the equilibrium boundary, and tend to decrease with pH (Fig. 4). There will be no hydroxide precipitate at pH = 14, and the main Pb compound in solution is the highly stable complex $Pb(OH)_3^-$ (solid line Pb(OH,L)) which consumes all the $Pb(OH)_2$ precipitate. The yield is almost independent of the initial oxalic acid value, since the later contributes mainly to the formation of $C_2O_4^{2-}$; the concentration of $H_2C_2O_4$ in the solution, about 10^{-20} mol l^{-1}, is neglected in Fig. 4. In these basic pH conditions, the concentration of the different $Pb(L)_i$ is greatly decreasing with pH.

If $[H_2L]_0 > \sum$L[H, Pb], and $[Pb]_o$ is too low (pH < 9·15 in our example), then the precipitation of PbC_2O_4 is the main reaction (area C in Fig. 3). This appears in acidic conditions and is dependent on the $[Pb]_o$value; also, the stability domains of $\sum$L[H, Pb] and Pb[H, L] should change with $[Pb]_0$ changes. Figure 5 presents the new domain of stability of the soluble species versus pH when $[Pb]_0$ is 0·07 mol l^{-1}. The oxalic acid contributes to two competitive reactions: by one hand there is the formation of Pb precipitate, with very high yield (> 99%), but, by the other hand, there is the formation of lead free complexes, which is only the residue of the first reaction. Following the acid dissociation of oxalic acid versus pH, a wide variation in the concentration of the different

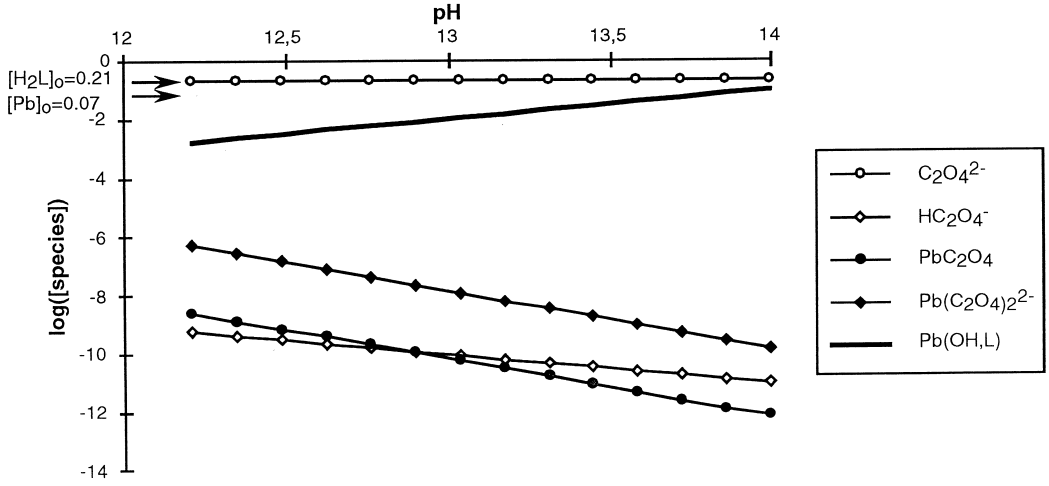

Fig. 4. Stability diagram for complexes formation in the Pb–oxalic acid–H_2O system, out of equilibrium ($[H_2L]_0 < \Sigma\ L(H,Pb)_{equ.}$).

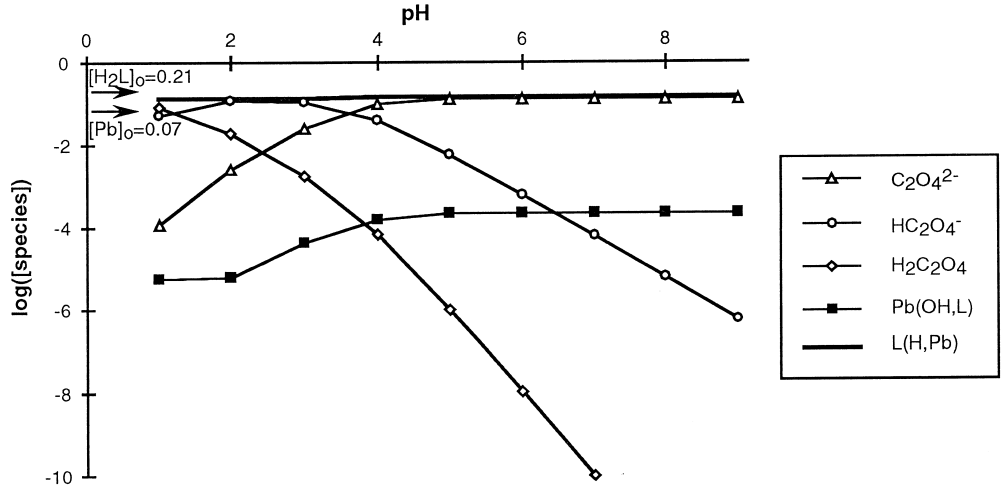

Fig. 5. Hydroxide precipitation yield profile out of equilibrium ($[Pb]_0 < \Sigma\ Pb(OH)_{equ.}$).

species is shown in the diagram. The uncommon shape of the Pb(OH,L) curve is due to predominant formation of Pb^{2+} at low pH, while, at higher pH, the later reacts to give PbC_2O_4 and $Pb(C_2O_4)_2{}^{2-}$.

3.3 La^{3+} aqueous solution

3.3.1 Hydroxide precipitation

Figure 6 shows the stability of the different lanthanum based hydroxide species in aqueous solution, derived in the same way as in the Pb case. $La(OH)_3$ precipitate presents an amphoteric behaviour with a wide stability range, from pH = 8·8 to 11, and tends to dissolve slighter than $Pb(OH)_2$, with the formation of hydroxo complexes as pH increases. For $La_o = 0{\cdot}006$ mol l^{-1} for example, it starts to precipitate at pH = 7·3, and continues in the highly basic zone. For pH values greater than 11, its solubility increases by the formation of $La(OH)_4{}^-$ complexes, whereas in acidic conditions, La^{3+} is the main soluble compound in the aqueous solutions.

3.3.2 Oxalate precipitation

Addition of oxalic acid ($[H_2L]_0 = 0{\cdot}21$ mol l^{-1}) modifies the previous diagram by creating an oxalate precipitation area (pH = 7·2–8·4), a mixed oxalate–hydroxide one (pH = 8·4–9·9), and a reduced hydroxide one (pH = 9·9–11·2) (Fig. 7). With lanthanum, the oxalate ions lead essentially to the formation of $La(C_2O_4)_3{}^{3-}$, at high pH values, which contributes to the increase of the solubility of $La(OH)_3$ precipitate, and then to develop its amphoteric behaviour. The dissociation of the precipitate $La_2(C_2O_4)_3$ is then complete at pH = 10–11, whereas at low pH, the low ratio of $C_2O_4{}^{2-}$ induces immediately the complex formation with La^{3+}, mainly $LaC_2O_4{}^+$.

In our given example, if actual chemical conditions are in the precipitation zone, then the precipitation profiles can be presented for different initial concentrations of $[La]_0$ and $[H_2L]_0$ (Fig. 8). In this case, the concentration $[H_2L]_0$ is chosen in accordance with the stoichiometric values ($[H_2L]_0 = 0{\cdot}09$ mol l^{-1}). High precipitation yield are reached either in oxalate form or in hydroxide one.

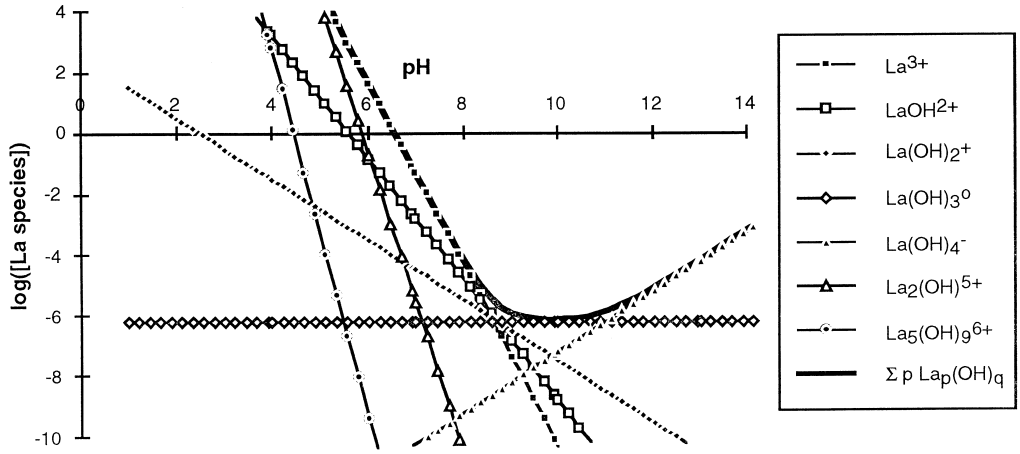

Fig. 6. Stability diagram for complexes formation in the La–H_2O system.

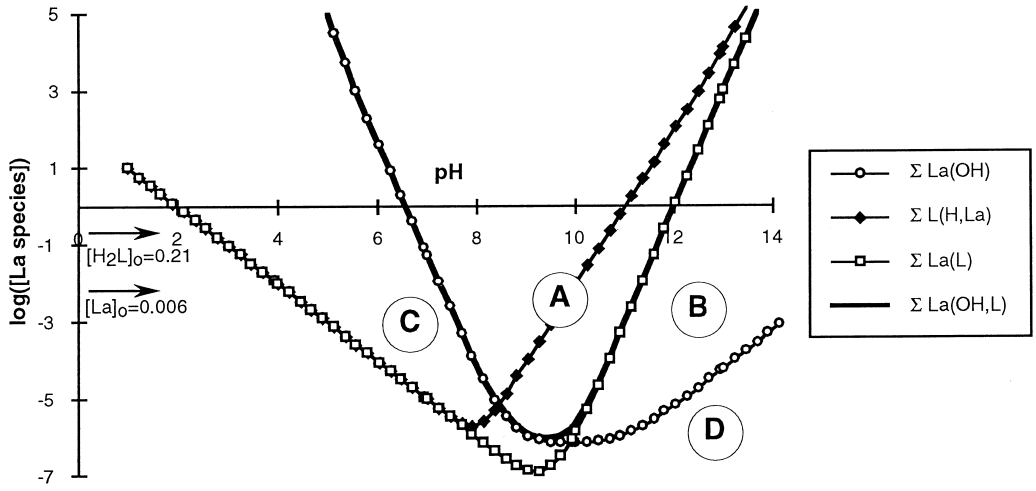

Fig. 7. Stability diagram for complexes formation in the La–oxalic acid–H_2O system.

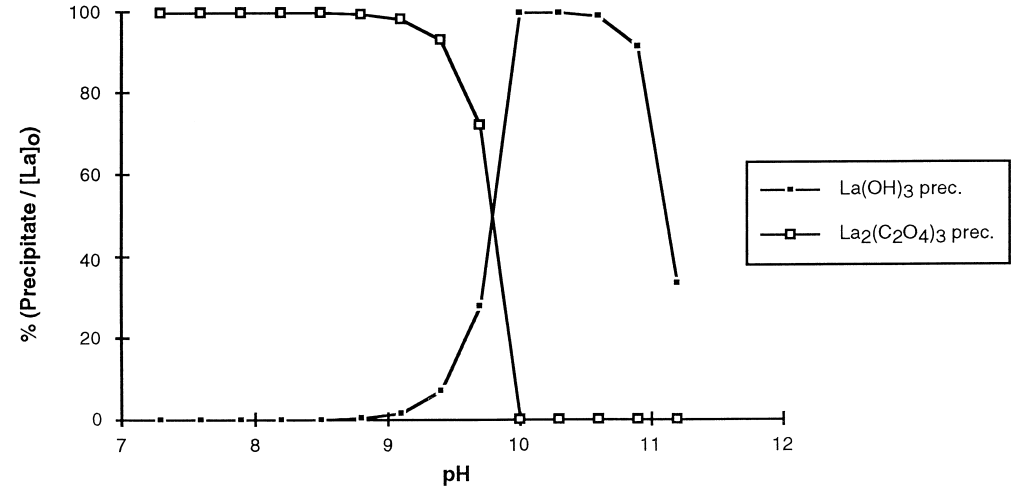

Fig. 8. Precipitation profiles in the La–oxalic acid–H_2O system, under equilibrium conditions (molar ratios).

3.3.3 Out of dual precipitation equilibrium

In the case where $[La]_0 > \sum La[OH]$, but with insufficient $[H_2L]_0$ (11·7 < pH < 14 in our example), which is in the basic zone of Fig. 7, the only solid formed is $La(OH)_3$. The latter is produced with high yield (Fig. 9) since the oxalic acid is transformed mainly into $C_2O_4^{2-}$, the stable species at high pH. By increasing pH, a light formation of hydroxo complexes, essentially $La(OH)_4^-$, occurs, whereas the hydroxide precipitate is slightly dissolved. The concentration of the hydroxide species is given by Fig. 6, as directly dependent on the OH^- concentration, via equilibrium (A3).

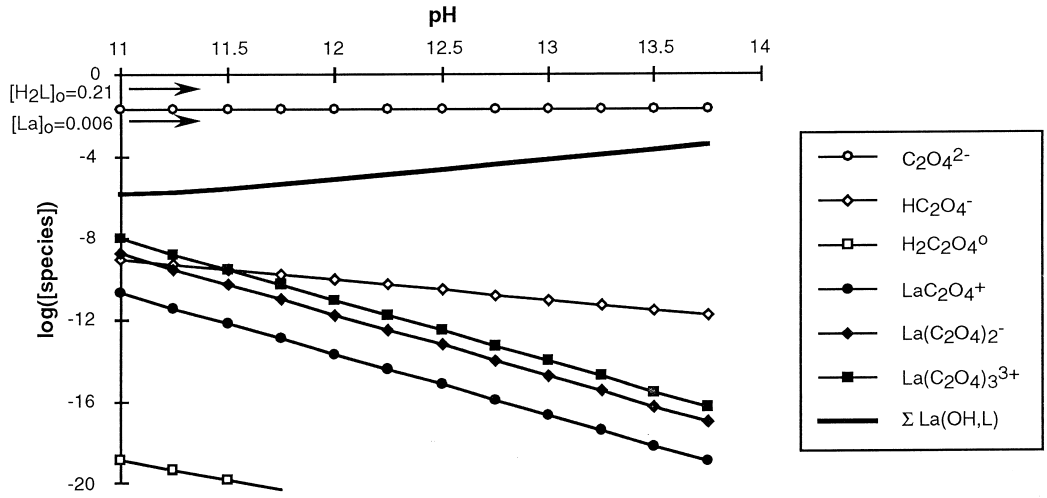

Fig. 9. Stability diagram for complexes formation in the La–oxalic acid–H_2O system, out of equilibrium ($[H_2L]_0 < \Sigma L(H,La)_{equ.}$).

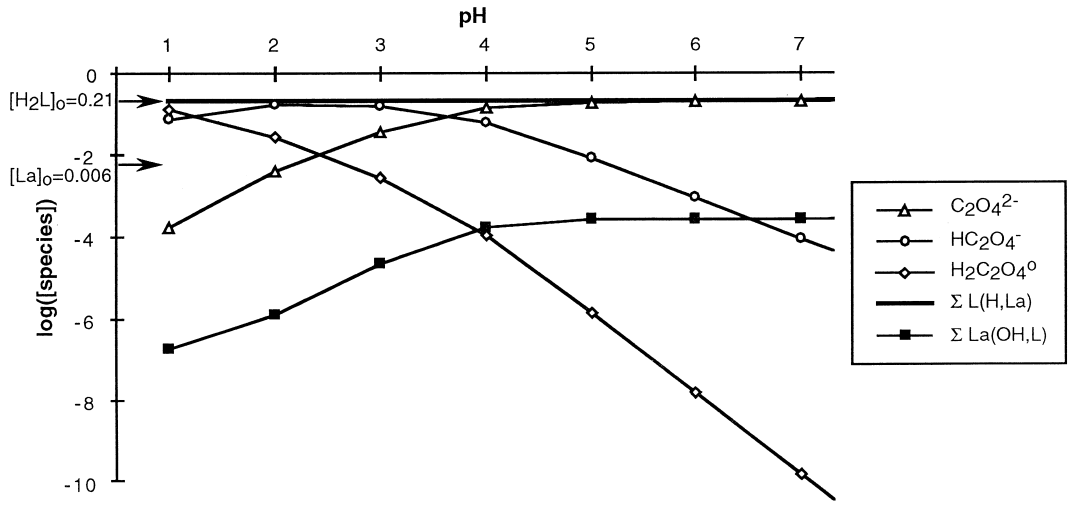

Fig. 10. Distribution profiles of the major soluble species in the La–oxalic acid–H_2O system, out of equilibrium ($[La]_0 < \Sigma La(OH)_{equ.}$).

As expected, the ratio of oxalate complexes decreases as pH increases, because $C_2O_4^{2-}$ does not reach its equilibrium concentration.

If $[H_2L]_0 > \sum L[H,La]$, and $[La]_0$ is too low (2·65 < pH < 7·3 in our example), quantitative precipitation (> 99% of $[La]_0$) of $La_2(C_2O_4)_3$ can be achieved (Fig. 10). The oxalate and hydroxide complexes concentrations are different from the equilibrium since they depend especially on the initial $[La]_0$. The main resulting components in the aqueous solution are the base forms of the oxalic acid, while a minor quantity of La complexes ($La(C_2O_4)_2^-$ and $La(C_2O_4)_3^{3-}$) is formed. Their concentration increases with pH, since the dissociation of the oxalic acid, in excess, is complete. As oxalate species are formed, there is a consumption of La^{3+}, the only stable metal species in the acidic conditions (Fig. 7).

3.4 Zr^{4+} aqueous solution

In a solution where only the OH^- concentration is modified, Zr^{4+} forms several complexes stable in the acidic zone, such as $Zr_4(OH)_8^{8+}$, $Zr(OH)_2^{2+}$, and $Zr(OH)_4^0$ (Fig. 11). At higher pH values (pH > 6), the major soluble species issued from Zr^{4+} is $Zr(OH)_5^-$.

The hydroxide precipitate $Zr(OH)_4$ also presents an amphoteric behaviour. This precipitate is very stable, considering that, for pH = 5–6, the concentration of Zr species is about 10^{-11} mol l^{-1}

Since there is no formation of a precipitate with $C_2O_4^{2-}$ (Table 1), the calculation of the different soluble species has been done considering only the hydroxide precipitation. The oxalate complexes, present in the solution if one add oxalic acid, were determined considering $[H_2L]_0 = 0{\cdot}21$ mol l^{-1}. In these conditions, the stability behaviour of $Zr(OH)_{4\ prec.}$ is presented in Fig. 12. The hydroxide curve is modified only in the acidic region because of the important formation of oxalate Zr-complexes. As pH increases, the decomposition of the oxalate complexes occurs with formation of acidic species $HC_2O_4^-$, then the latter dissociates completely into the more stable $C_2O_4^{2-}$, which reaches the concentration of $[H_2L]_0$ (Fig. 13).

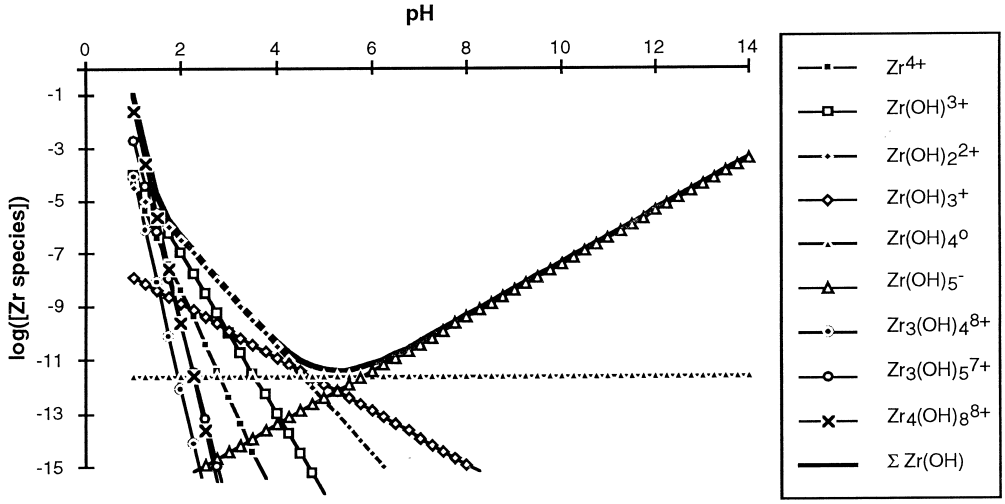

Fig. 11. Stability diagram for complexes formation in the Zr–H_2O system.

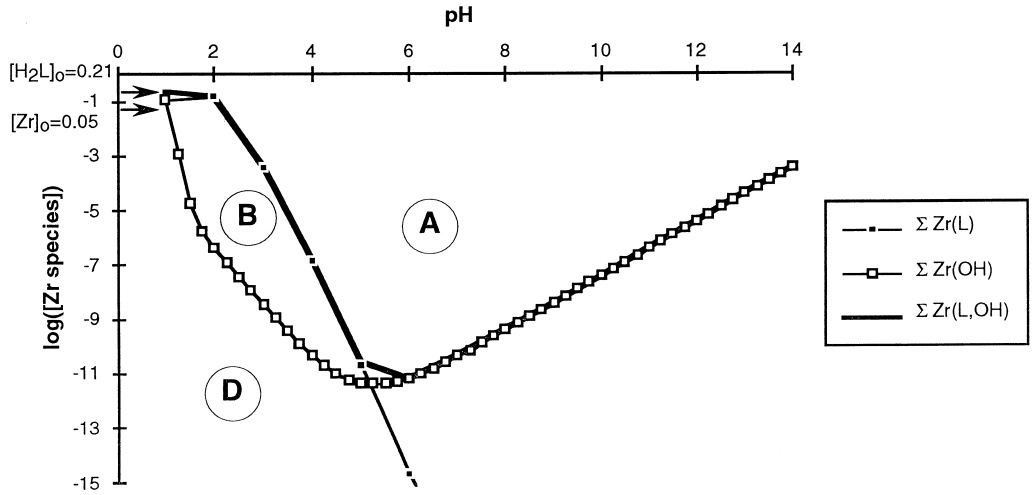

Fig. 12. Stability diagram for complexes formation in the Zr–oxalic acid–H_2O system.

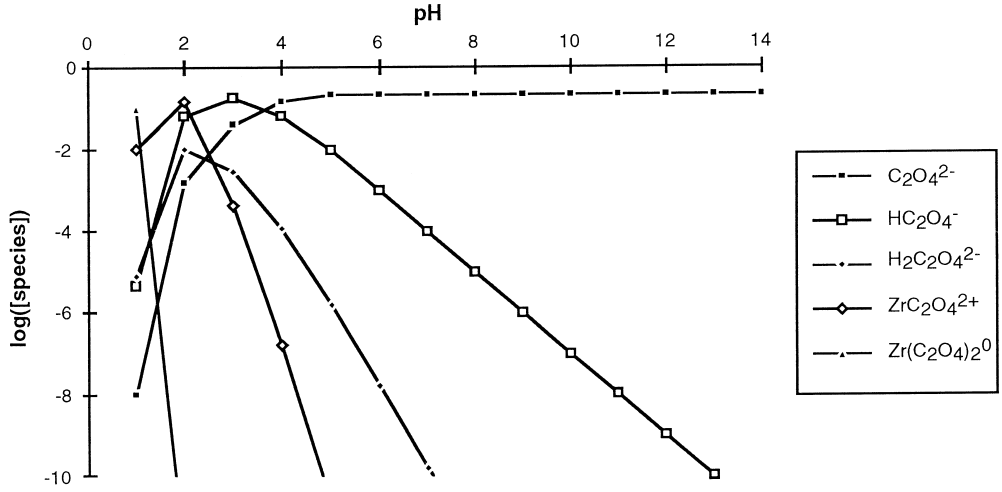

Fig. 13. Distribution profiles of the different soluble species, deriving from oxalic acid, in the Zr–oxalic acid–H_2O system.

3.5 Ti^{4+} aqueous solution

Some authors,[27] working on Ti based aqueous solutions, reported that Ti^{4+} is only stable at very low pH (pH < 0·32) and that, for higher pH value, the species stable is TiO^{2+} (pH > 0·65). Consequently to avoid this problem, all the constants given in Table 1 take into account only the TiO^{2+} formation.

By adjusting the pH in a solution of TiO^{2+}, the precipitation of $TiO(OH)_2$ can occur with high yield at pH value as low as 3 (Fig. 14). This precipitation ratio, and the hydroxide solubility are

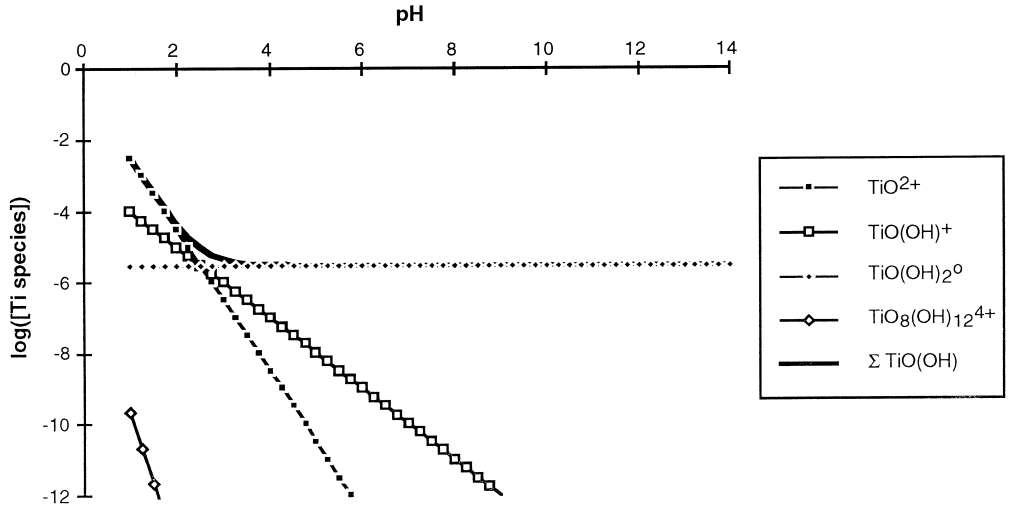

Fig. 14. Stability diagram for complexes formation in the Ti–H_2O system.

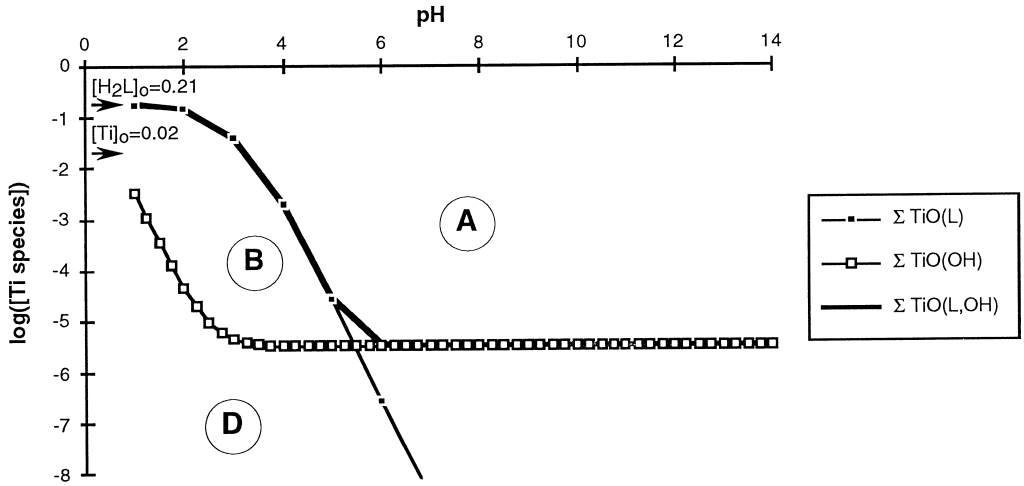

Fig. 15. Stability diagram for complexes formation in the Ti–oxalic acid–H_2O system.

constant whatever the pH value imposed. Apart the $TiO(OH)_2^0$ complex, no other one is reported to be present in the basic domain. However, as indicated in Table 1, few data about complexes formation of TiO^{2+} and OH^- are available till now.

By addition of oxalic acid ($[H_2L]_0 = 0{\cdot}21\ mol\,l^{-1}$), as in the case of Zr^{4+}, the formation of oxalate complexes in acidic pH, modifies the stability domain of $TiO(OH)_2$ (Fig. 15). Increasing the pH value, the oxalate complexes followed the same decomposition behaviour as the one already reported for $Zr(OH)_4$, except that there is a complex, $TiO(C_2O_4)$, which is very stable in acidic conditions (pH < 2·5) (Fig. 16).

4 Experimental Procedure

4.1 Coprecipitation of the metal ions solutions

$Pb(NO_3)_2$ (Carlo Erba, 99·5%), $La(NO_3)_3$, $6H_2O$ (Merck, 99%), $TiCl_4$ (Merck, 99%), $ZrO(NO_3)_2$, xH_2O, (Aldrich, purity not available. ICP analysis of the as-received powder performed in our laboratory gives the following formula $ZrO(NO_3)_2$, $2.2H_2O$), $H_2C_2O_4$, $2H_2O$ (Riedel-de Haen, 99·5%) were used as starting materials.

Because of the low relative permittivity of ethanol compared to that of water, 24·3 versus 81, respectively,[30] this solvent has been sometimes preferred in order to decrease the precipitate solubility. In our experiments, water and alcohol (98%) lead to equivalent precipitation yields, and no unexpected aqueous combination with the metal ions was detected. The necessary amount of the different nitrate salts was dissolved separately with a quantity of water sufficient to reach a clear solution at room temperature. The aqueous solution of titanium has been directly prepared, by adding deionized water to $TiCl_4$ at $\approx 4°C$.

An aqueous solution of oxalic acid, containing usually the corresponding stoichiometry for individual reactions with each ion (i.e. $C_2O_4^{2-} = 1 \times Pb^{2+}$, or $1{\cdot}5 \times La^{3+}$, or $2 \times Zr^{4+}$, or $2 \times Ti^{4+}$) was also prepared.

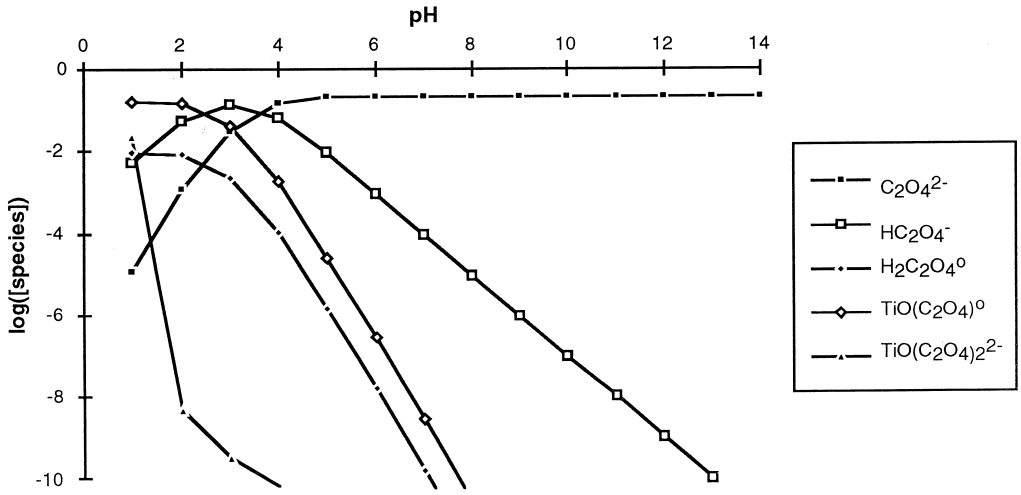

Fig. 16. Distribution profiles of the different soluble species, deriving from oxalic acid, in the Ti–oxalic acid–H_2O system.

Deionized water was then added in order to get the required concentration. The precipitation was achieved by mixing the individual metal solutions with the oxalic acid one, under magnetic stirring, at room temperature. Usually, pH was adjusted with NH_4OH 3M (starting from Riedel-de Haen, 25%). In order to make some verifications, NaOH 1M (Merck) was occasionally used.

For the different calculations, the following concentrations, $[Pb]_0 = 0{\cdot}07\,mol\,l^{-1}$, $[La]_0 = 0{\cdot}006\,mol\,l^{-1}$, $[Zr]_0 = 0{\cdot}05\,mol\,l^{-1}$, $[Ti]_0 = 0{\cdot}02\,mol\,l^{-1}$, $[H_2C_2O_4]_0 = 0{\cdot}21\,mol\,l^{-1}$, were chosen in order to foreshadow, in each individual solution, the final solution for PLZT 8/65/35 preparation.

4.2 Powder characterization

The resulting powders were characterized by X-rays diffraction (XRD) (Rigaku Geigerflex D/max-IIVC (2·0 kW)) using Ni filtered CuK_α radiation. In the case of lead free powders, to obtain more details on the mechanisms of precursor decomposition, thermogravimetric analysis (TGA) (Linseis L81/042C) was carried out at a heating rate of 5°C min^{-1}, in air, in the temperature range 25–1000°C.

5 Results and Discussion

5.1 Preparation of Pb-oxalates

In order to confirm the results of the calculation, Pb^{2+}-oxalic acid solutions were prepared at various pH conditions. The resulting X-rays diffraction spectra with pH = 1 and pH = 10 are presented in Fig. 17. At pH = 1, for $[Pb]_0 = 0{\cdot}2\,mol\,l^{-1}$, $[H_2C_2O_4]_0 = 0{\cdot}3\,mol\,l^{-1}$, the resulting dried precipitate gives exactly the same diffraction pattern as PbC_2O_4 (JCPDS card no. 14-803). The lead ions in oxalic acid solution behave as previously anticipated by the calculation (Fig. 3). In these pH conditions, whatever is initial concentration, the precipitation yield of PbC_2O_4 (controlled by

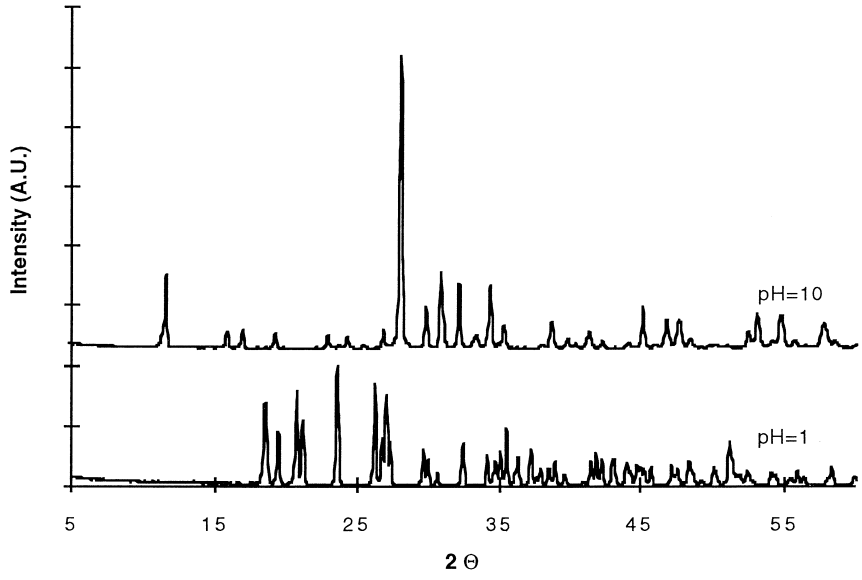

Fig. 17. XRD patterns for Ph based precipitates as a function of the pH of the initial solution.

weighting the final product) is always higher than 99%.

For the precipitates obtained in the pH range 10–12·9, the dried powders exhibit always the same crystalline pattern (Fig. 17). According to the calculations (cf. Section 3.2), these powders should contain either $Pb(OH)_2$, for pH > 12 (Fig. 4), or a mixture of both $Pb(OH)_2$ and PbC_2O_4 for pH < 12, (Fig. 3), but none of these were detected by XRD (JCPDS cards 11-270 and 14-803, respectively). The precipitate obtained this pH range must be a particular phase with the two kinds of the anionic groups, i.e. a phase with the general formula

$$Pb(OH)_x(C_2O_4)_{1-x/2} \quad \text{with } 0 < x < 2 \qquad (6)$$

Taking the powder obtained at pH = 10, for $[Pb]_0 = 0{\cdot}07\,mol\,l^{-1}$ and $[H_2C_2O_4]_0 = 0.1\,mol\,l^{-1}$, and heating it up to 850°C, one obtains PbO as the only present phase (revealed by XRD), with a yield of 83·9%. The powder molar weight was then calculated to be $266{\cdot}07\,g\,mol^{-1}$, which gives

$$Pb(OH)_{1.07}(C_2O_4)_{0.46} \approx Pb_2(OH)_2(C_2O_4) \qquad (7)$$

TGA curve of this compound (Fig. 18) shows a continuous weight loss up to 850°C, with a pronounced step from 340 to 390°C. If the weight loss from room temperature up to 340°C corresponds to the evolution of water from the material, it should be 3·65% according to eqn (7), which is in good agreement with the experimental result, ≈3·6%. However. it must be pointed out that the precipitate seems to be a new compound, further work is necessary to better characterize it. In the literature, there is no evidence of this compound, Wilson *et al.*,[32] in other experimental conditions (using ethyl alcohol as solvent), only found an amorphous compound, with an established formula of $Pb_3(OH)_2(C_2O_4)_2$. In these basic conditions (pH > 10), as pH increases, there is a decrease of the precipitate formation (Fig. 19) in agreement with the previous calculations of the solubility versus pH.

Because of the lack of data, this phase couldn't be introduced in the diagrams (Figs 3 and 4). However this should not create a great alteration in the different areas in these figures, since it only changes the solid phase composition deriving from the complexes formation.

5.2 Preparation of the La-oxalates

The precipitation of La-oxalate compound was driven in each part of the stability diagram in order to determine the phase formation. In acidic conditions (pH = 1), a white feathery precipitate was formed which presents high crystallinity after filtering and drying. The precipitation of this compound is not in agreement with the results of the calculations because $[La]_0$ $(0{\cdot}004\,mol\,l^{-1})$ and $[H_2C_2O_4]_0$ $(0{\cdot}075 mol^{-1})$ are out of the equilibrium conditions, i.e. no precipitate should be formed. This can be explained by the lack of accuracy in the measurement of the complexes stability constants in very high concentrated solutions. Another possible explanation is given by Martell *et al.*:[29] for pH < 2 or pH > 12, accurate hydrogen ion concentration (or activity) cannot be measured with glass electrode–reference electrode systems because the liquid junction potentials changes as pH is modified. Then, the measured pH shouldn't be correct since for the pHmeter, by giving buffer solutions on starting the measurement, a linear variation of the potential versus pH has been considered.

The XRD pattern of this precipitate (Fig. 20) presents different characteristics from the only known phase, $La_2(C_2O_4)_3$, $10H_2O$, reported in the JCPDS card no. 20-549. A thermogravimetric analysis of the material, in the range 25–1000°C

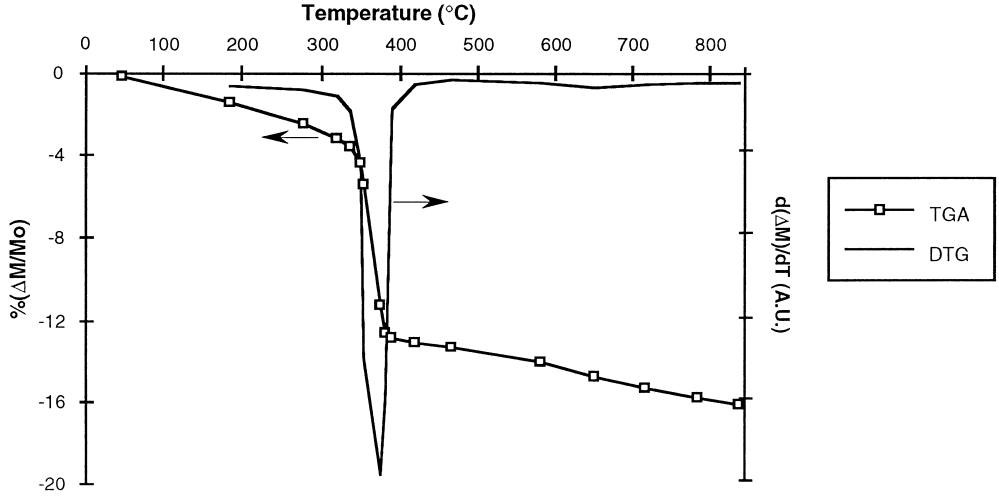

Fig. 18. TGA and DTG profiles of $Pb(OH)_x(C_2O_4)_y$ product obtained at pH = 10.

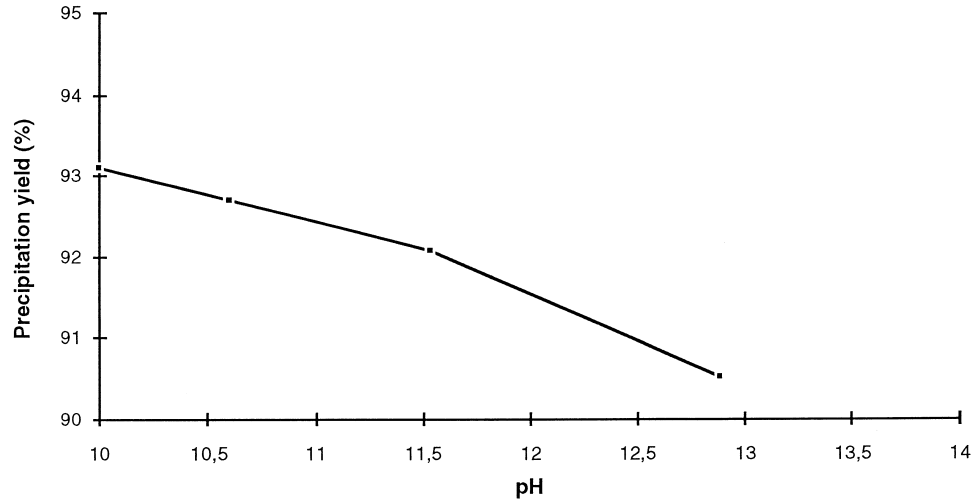

Fig. 19. Precipitation yield of $Pb(OH)_x(C_2O_4)_y$ as a function of the pH of the initial solution.

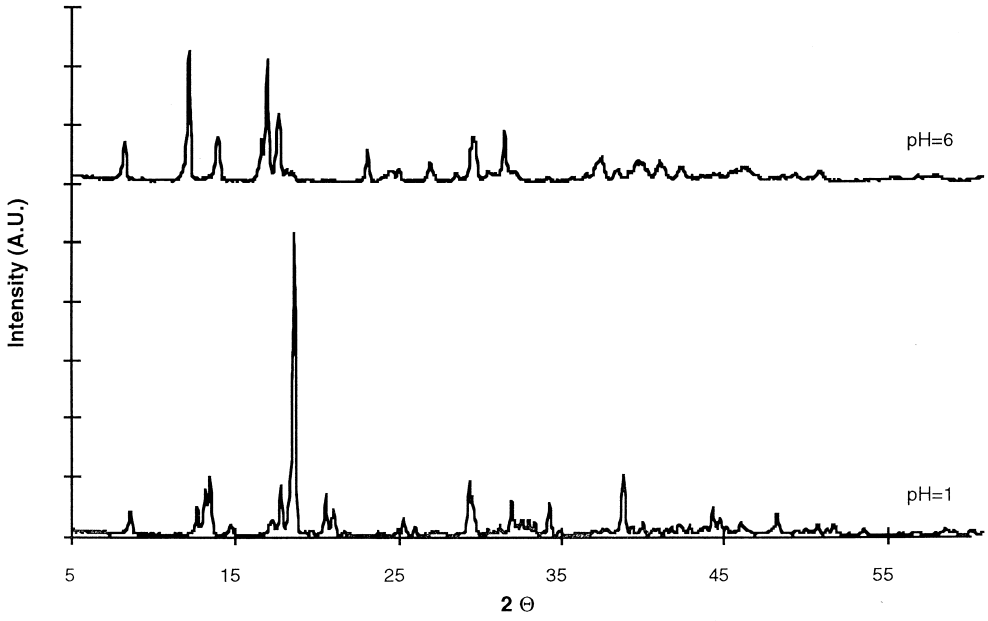

Fig. 20. XRD patterns for La based precipitates as a function of the pH of the initial solution.

[Fig. 21(a)], allows to establish the following chemical formula:

$$La_2(C_2O_4)_3, 9{\cdot}15H_2O \qquad (8)$$

This formula was calculated taking into account that the high temperature residue is the stable oxide phase, La_2O_3, which was confirmed by XRD (JCPDS card no. 5-602). The different results given by TGA are presented in Table 2.

The separation between $La_2O(CO_3)_2$ and La_2CO_5 is not clear since there is no dwell in the TGA curve. Then, the existence of these two phases can only be inferred by the DTG results.

Modifying the pH towards a more basic solution, pH = 6, by adding of NH_4OH, a white expected precipitate appears, but its yield is higher than the theoretical oxalate one, which indicates that the new precipitate has a different composition. This precipitate can be formed in the pH range 6 to 9. Dried at 60°C, it could not be identified on the basis of the JCPDS files already existing. This phase is not the same as the one obtained at pH = 1 (Fig. 20), and the only difference in both preparation is the presence of NH_4OH in the precipitation medium, added to raise the pH in the solution up

Table 2. Summary of thermal analysis of lanthanum oxalate

T (°C)	*Weight loss (%)*		*Residue*
	Observed	*Calculated*	
25	0	0	$La_2(C_2O_4)_3$, $9H_2O$
327	23·07	23·03	$La_2(C_2O_4)_3$
476	44·06	41·21	$La_2O(CO_3)_2$
558	46·87	47·47	La_2CO_5
1000	54·43	53·72	La_2O_3

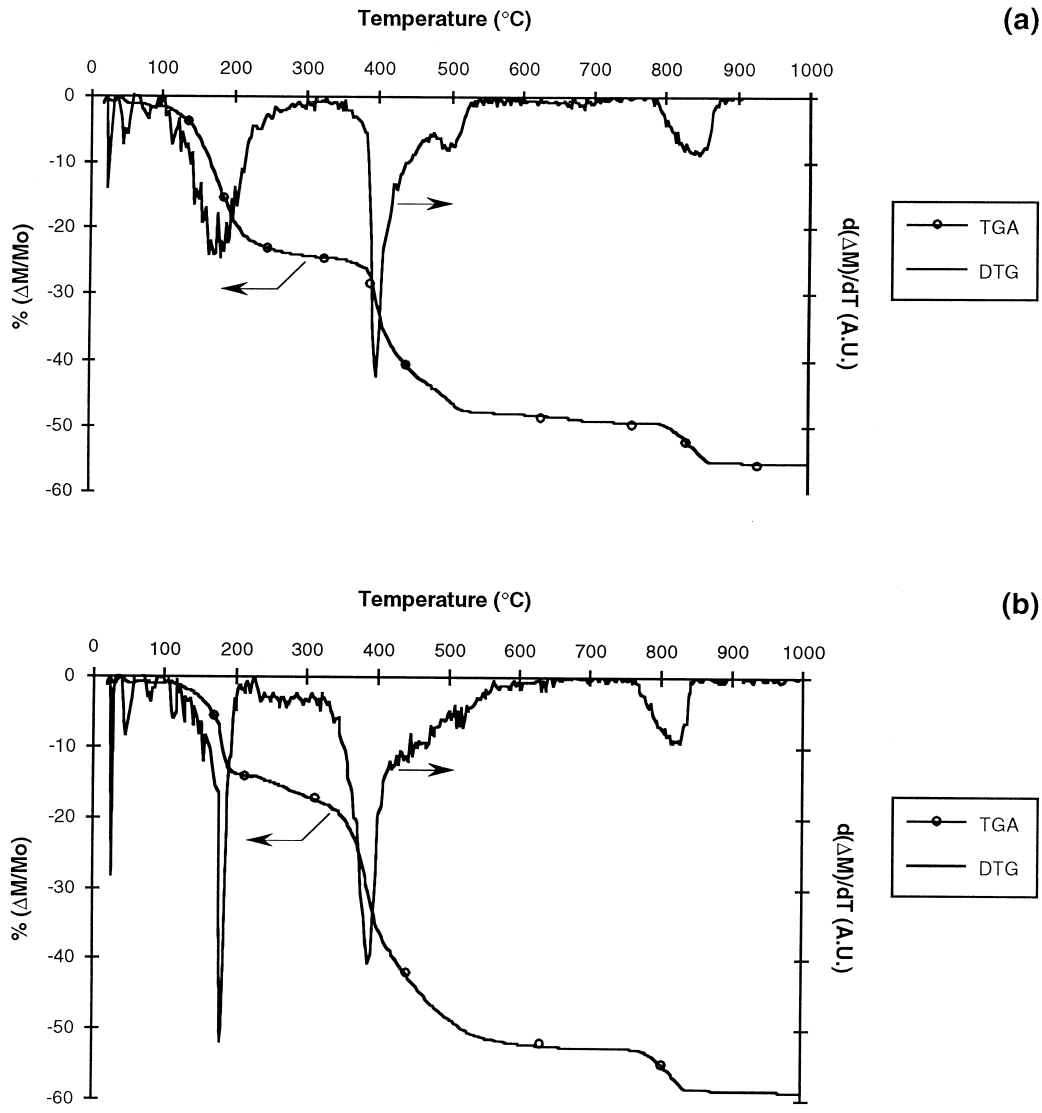

Fig. 21. TGA profiles of La precipitates under air, as a function of the pH of the initial solution (a) pH = 1, (b) pH = 6.

to 6. The higher yield obtained at this pH could arise from the incorporation of NH_4^+ species into the precipitate, according to the general formula:

$$La_2(C_2O_4)_x(NH_4)_{2x-6,}\, yH_2O \qquad (9)$$

This kind of oxalate–ammonium mixed compound has already been reported by some authors in the case of lanthanides and actinides compounds, like Lu $(C_2O_4)_2$ (NH_4), H_2O[33] and $Th_2(C_2O_4)_6$ $(NH_4)_4$, $7H_2O$.[34] FTIR performed on the powder obtained at pH = 6, Fig. 22 shows that, together with the spectral bands characteristics of lanthanum oxalate, it is confirmed the presence of ammonium in the molecule by the peaks at 1401 and 3212 cm^{-1}.[35,36] To further check the possibility of the ammonium incorporation in the new phase, NaOH was used to raise the pH of a new solution, instead of NH_4OH. In his condition, a precipitate is formed which seems to be the mixture of La nitrate and Na oxalate, while the previous phase obtained in the presence of NH_4OH was prevented.

By TGA, comparing the two lanthanum precipitates, Fig. 21(a) and (b), a higher global decomposition step ($\approx -14{\cdot}8\%$) is detected in the range 350–500°C for the basic precipitate, which allows the assumption that it is richer in oxalate groups. Also, by DTG, in Fig. 21(b), a new decomposition step ($\approx 3{\cdot}36\%$) seems to be located from 220 to 314°C. Considering the final yield (41·51%) and assuming that the residue at 1000°C is only composed by La_2O_3 (the only detected phase by XRD), the following formula was established considering the possible reaction between NH_4^+ and $(C_2O_4)^{2-}$

$$La_2(NH_4)_{2.19}(C_2O_4)_{4.09},\ 5.93H_2O \approx La(NH_4)(C_2O_4)_2,\ 3H_2O \qquad (10)$$

If the weight loss from 220 to 320°C corresponds to the evolution of NH_3 from the material, it

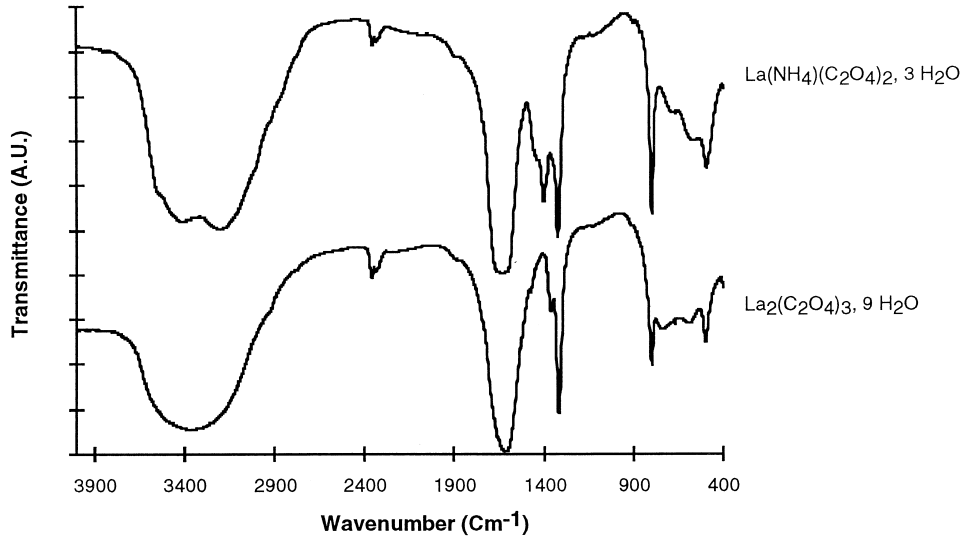

Fig. 22. FTIR spectra for the two kind of La precipitates.

should be about 4·72%, taking into account the chemical formula (10) which is in quite good agreement with the experimental result, $\approx 3{\cdot}36\%$. This temperature range for the evolution of ammonia has already been reported for silazanes.[35]

5.3 Zr–Ti–acid oxalic system

For Zr^{4+} and TiO^{2+}, no solubility product was available in the different compilations used (cf. Sections 3.4 and 3.5). Moreover, we did not manage to get any precipitate after mixing the oxalic acid and the aqueous solutions of these metals, in the acidic conditions. The only precipitates were obtained in basic conditions, by reaction with the OH– anions.

Concerning the formation of Ti–OH complexes in the basic domain, the presence of Ti in the supernatant solution was detected by titration up to pH = 8; this means that an unidentified complex is present in the solution which tend to disappear at high pH. This observation, which is in agreement with the results of Fox *et al.*[37] leads to some discrepancy with the calculated curve (Fig. 14) where the Ti-complex concentration seems to remain constant with pH, whereas it should decrease.

6 Conclusion

In order to define the optimum conditions for the preparation of a PLZT oxalate precursor, the different stability domains, based on the equilibrium constants of the complexes formation, have been determined for each individual component of PLZT. The precipitation of metal ion is strictly dependent on the ionic concentration and on the pH of the solution. Then, experimental conditions have been chosen in order to produce and separate the precipitate phases and to control the precipitation yield.

Experiments brought quite good confirmation to the previous calculations. The only limitation is originated by the compilations of stability constants which are still incomplete in mixed ligand data. By modifying the pH conditions, the preparation of several new metal-oxalate has been reported. This new compounds have been characterized by several techniques of analysis (TGA, FTIR, XRD). These results given for individual components should be of great interest in order to prepare the mixed metal ion solution for PLZT precursor synthesis.

Acknowledgements

One of the authors, M. Pereira, acknowledges the support of the Portuguese Research Council, JNICT, under the Praxis XXI program, for the grant no. BPD/992/94, and the INESC, under the project 'Optosensores'. Special thanks also to Dr Gilberto Vasco for help with FTIR measurements.

References

1. Herbert, J. M. *Ferroelectric Transducers and Sensors*, Vol. 3. Gordon and Breach Science, 1985, pp. 6–155.
2. Härdtl, K. H. and Hennings, D., Distribution of A-site and B-site vacancies in (Pb,La) $(Ti,Zr)O_3$ ceramics. *J. Am. Ceram. Soc.*, 1972, **55**(5), 230.
3. Haertling, G. H. and Land, C. E., Hot pressed (Pb, La)$(Zr,Ti)O_3$ ferroelectric ceramics for electrooptic applications. *J. Am. Ceram. Soc.*, 1971, **54**(1), 1.
4. Okazaki, K. and Nagata, K., Effects of the grain size and porosity on electrical and optical properties of PLZT ceramics. *J. Am. Ceram. Soc.*, 1973, **56**(2), 82.

5. Bradley, F. N., Discussion of 'Effects of the grain size and porosity on electrical and optical properties of PLZT ceramics'. *J. Am Ceram. Soc*., 1973, **56**(7), 404.
6. James, A. D. and Messer, P. M., The preparation of transparent PLZT ceramics from oxide powders by liquid sintering. *Trans. Br. Ceram. Soc*., 1978, **77**, 152.
7. Matsuyama, I. and Jyomura, S., Grain size dependence of optical transmission in 7.6/70/30. *J. Am. Ceram. Soc*., 1975, **58**(7–8), 347.
8. Bahloul, X. D., Pereira, M. and Goursat, P., Preparation of silicon carbonitrides from an organosilicon polymer: II, Thermal behavior at high temperatures under argon. *J. Am. Ceram. Soc*., 1993, **76**(5), 1163.
9. Brown, L. M. and Mazdiyasni, K. S., Cold pressing and low temperature sintering of alkoxy-derived PLZT. *J. Am. Ceram. Soc*., 1972, **55**(11), 541.
10. Kleer, G. and Schmitt, H., The grain size of mixed oxide and chemically prepared PLZT-powders. *Mater. Res. Bull*., 1981, **16**(12), 1541.
11. Colomban, P., Frittage de céramiques transparentes PLZT 9/65/35. *Indus. Céram*, 1976, **697**(7–8), 531.
12. Little, J. A. and Yao, P. C., Microscopic characterization of $Pb_{0.91}$ $La_{0.09}$ $(Zr_{0.65}$ $Ti_{0.35})_{0.98}$ O_3. *J. Am. Ceram. Soc*., 1984, **67**(2), C29.
13. Duran, P. and Moure, C., High density PLZT ceramics prepared chemically from different raw materials. *Am. Ceram. Soc. Bull*., 1985, **64**(4), 575.
14. Lin, W. K., Jou, M. S. and Chang, V. H., Chemical preparation of PLZT powders by the carbonate method. *Ceram Int*., 1988, **14**, 223.
15. Murata, M., Wakino, K., Tanaka, K. and Hamakawa, Y., Chemical preparation of PLZT powder from aqueous solution. *Mat. Res. Bull*., 1976, **11**, 323.
16. Yoshikawa, Y. and Tsuzuki, K., Susceptibility to agglomeration of fine PLZT powders prepared from nitrate solutions. *J. Europ. Ceram. Soc*., 1990, **6**, 227.
17. Thomson Jr, J., Chemical preparation of PLZT powders from aqueous nitrate solutions. *Am. Ceram. Soc. Bull*., 1974, **53**(5), 421.
18. Akbas, M. A. and Lee, W. E., Synthesis and sintering of PLZT powder made by freeze/alcohol drying or gelation of citrate solutions. *J. Europ. Ceram. Soc*., 1995, **15**, 57.
19. Clabaugh, W. S., Swiggard, E. M. and Gilchrist, R., Preparation of baryum titanyl oxalate tetrahydrate for conversion to baryum titanate of high purity. *J. Res. Nat. Bur. Stand (US)*, 1956, **56**, 289.
20. Gallagher, P. K., Schrey, F. and Dimarcello, F. V., Preparation of semiconducting titanates by chemical methods. *J. Am. Ceram. Soc*., 1965, **46**(8), 301–405.
21. Saegusa, K., Rhine, W. E. and Bowen, H. K., Preparation of stoichiometric fine lead barium titanate powder. *J. Am. Ceram. Soc*., 1993, **7**(6), 1495.
22. Yamamura, H., Tanada, M., Haneda, H., Shirasaki, S. and Moriyoshi, Y., Preparation of PLZT by oxalate method in ethanol solution. *Ceram. Int*., 1985, **11**(1), 23.
23. Song, B. M., Kim, D. Y. and Yamamura, H., Complete precipitation of PLZT oxalate by ammonia addition. *Ceram. Int*., 1986, **12**, 179.
24. Choy, J. H., Han, Y. S. and Kim, J. T., Hydroxide coprecipitation route to the piczoelectric oxide Pb(Zr, Ti)O_3 (PZT). *J. Mater. Chem*., 1995, **5**(1), 65–69.
25. Kratgen, J., *Atlas of Metal–Ligand Equilibria in Aqueous Solution*. Series in Analytical Chemistry, Ellis Horwood, Chichester, UK, 1978.
26. Sillen, L. G. and Martell, A. E., *Stability Constants of Metal–Ion Complexes* Suppl. 1, Special publ. 25. The Chemical Society, London, 1971.
27. Högfeldt, E., *Stability Constants of Metal–Ion Complexes, Part A, Inorganic Ligands*. IUPAC Chemical Data Series, no. 21, Pergamon Press Oxford, 1983.
28. Baes, C. F. and Mesmer, R. E. *The Hydrolysis of Cations*. Wiley, New York, 1976.
29. Martell, A. E. and Motekaitis, R. J., *Determination and Use of Stability Constants*, VCH, New York, 1988.
30. Pataki, L. and Zapp, E., *Basic Analytical Chemistry*, Vol. 2. Pergamon Press, Oxford, 1980.
31. Ringbom, A., *Les Complexes en Chimie Analytique*, Dunod, Paris, 1967, trans. from *Complexation in Analytical Chemistry*, Interscience, New York, 1963, Chap. II, pp. 20–43.
32. Wilson, O. C. and Riman, R. E., Morphology control of lead carboxylate powders via anionic substitutional effects. *J. Coll. Interf. Sci*., 1994, **167**, 358.
33. Barret *et al*., *J. Inorg. Nucl. Chem*., 1964, **26**, 931 in JCPDS card no. 19-735.
34. Bressot *et al*., *Bull. Soc. Chim Fr*., 1966, 2094 in JCPDS card no. 20-1271.
35. Pereira, M., PhD thesis, University of Limoges, France 1994.
36. Nakamoto, K., *Infrared and Raman Spectra of Inorganic and Coordination Compounds*, 4th edn. Wiley, New York, 1986, p. 131.
37. Fox, G. H., Adair, J. H. and Newnham, R. E., Effects of pH and H_2O_2 upon coprecipitated $PbTiO_3$ powders. Part I. Properties of as-precipitated powders. *J. Mater. Sci*., 1990, **25**, 3634.

Appendix

1 Theoretical Approach

In this step, we first check the pH area of stability of the different species which can be formed in an aqueous solution, and then the same will be applied for an oxalic modified solution. Some considerations must be done in order to validate the final results:

1. The ionic strength of the solutions has a limited influence on the stability constants since it is in the interval of 0·1 to 1.[30,31]
2. Since no constants for the mixed ligand complexes [i.e. $M(C_2O_4^{2-}-OH^-)$] nor for mixed metal complexes formation are available, these species will not be taken into account.
3. The diagrams are constructed based on thermodynamical data for the description of the equilibrium state, and no kinetic parameters have been taken into account. However, some reactions are known to be limited by kinetic parameters.[31]
4. In the case where precipitation occurs, the activity of the solid phase should be considered as equal to 1 since no interaction with the other phases can be possible.

1.1 Hydroxide formation

When a metal ion M^{n+} is added to an aqueous solution, the formation of various hydroxide species appears. The concentration of theses species depends on the pH of the solution and on total amount of M^{n+}, the initial concentration $[M^{n+}]_0$. We can express it by the general mass balance:

$$\begin{aligned}\left[M^{n+}\right]_0 = {} & \left[M^{n+}\right] + \left[M(OH)^{(n-1)+}\right] \\ & + \left[M(OH)_2^{(n-2)+}\right] + \left[M(OH)_3^{(n-3)+}\right] \\ & + \ldots + p\left[M_p(OH)q^{(np-q)+}\right] + \ldots + \\ & \left[(M(OH)_n)_{aq.}\right] + \left[(M(OH)_n)_{prec.}\right]\end{aligned} \tag{A1}$$

(For convenience, charges and brackets will be omitted in the next reactions.)

The system can now be described introducing the so-called Ringbom's[25,31] side-reaction coefficient $\alpha_{M(OH)}$, which considers the total concentration of the metal not involved in the formation of the precipitate $M(OH)_n$. $\alpha_{M(OH)}$ is then the ratio:

$$\begin{aligned}\alpha_{M(OH)} = {} & (M + M(OH) + M(OH)_2 + M(OH)_3 \\ & + \ldots + pM_p(OH)_q \\ & + \ldots + (M(OH)_n)_{aq.})/M\end{aligned} \tag{A2}$$

Now, considering the general reaction for complex formation, from M^{n+} and the OH^- ligand, including mono- and polynuclear complexes,

$$pM + qH_2O \Longleftrightarrow M_p(OH)_q + qH \tag{A3}$$

the law of mass action allows to write the equilibrium constant of the reaction as:

$$*\beta_{qp} = [M_p(OH)_q][H]^q/[M]^p \tag{A4}$$

If the metal ion M^{n+} can form a precipitate, it should have the composition of $M(OH)_n$. This compound only precipitates when its solubility is exceeded. The precipitate is then submitted to the solubility product, $*K_{SO}$, defined from the reverse of the above reaction (A4) as:

$$*K_{SO} = [M]/[H]^n \tag{A5}$$

At the equilibrium, by substitution of (A5) in (A4), one gets:

$$[Mp(OH)q] = *\beta qp \times [H]^{np-q} \times *K_{SO}^p \tag{A6}$$

and,

$$\begin{aligned}\log\left[pM_p(OH)_q\right] = {} & \log *\beta_{qp} - (np-q)pH \\ & + p\log(*K_{SO}) + \log p\end{aligned}$$

The side reaction species concentration versus pH can be written as:

$$M \times \alpha_{M(OH)} = \sum_{p,q} 10^{(\log *\beta qp - (np-q)pH + p\ log(*K_{SO}) + \log p)} \tag{A7}$$

This equation (A7) which is the sum of the concentrations of the soluble species at equilibrium, represents also the borderline of the metal–hydroxide precipitation. According to Ringbom,[31] the formation of a precipitate can often be considered as the final step of the polynuclear complexes formation by ionic aggregation and combination of those aggregates to form neutral compounds.

1.2 Oxalate precipitation

In order to verify the influence of the addition of oxalic acid on the hydroxide precipitation, Kratgen[25] has considered the quantity L′, which is the total amount of $C_2O_4^{2-}$ not bounded to the metal. The new side coefficient reaction is then defined as:

$$\begin{aligned}\alpha_{M(L,OH)} = {} & \alpha_{M(OH)} + (ML + ML_2 \\ & + \ldots + MH_iL_j + \ldots)/M\end{aligned} \tag{A8}$$

The MH_iL_j complexes were not considered since we found no accurate data available. The free species of this acid are well defined by the two acidity constants ($1/K_2$ and $1/K_1$). For this acid, dissolved alone in water, the distribution of the different species as a function of pH can be calculated as the solution of the following three equations:

$$[H_2C_2O_4]_0 = H_2C_2O_4 + HC_2O_4^- + C_2O_4^{2-} \tag{A9}$$

$$K_1 = \left[HC_2O_4^-\right]/[H]\left[C_2O_4^{2-}\right] \tag{A10}$$

$$K_2 = [H_2C_2O_4]/[H]\left[HC_2O_4^-\right] \tag{A11}$$

In fact,

$$C_2O_4^{2-}/(H_2C_2O_4)_0 = 1/\left(K_1K_2H^2 + K_1H + 1\right) \tag{A12}$$

$$HC_2O_4^-/(H_2C_2O_4)_0 = 1/(K_2H + (1/K_1H) + 1) \tag{A13}$$

$$\begin{aligned}H_2C_2O_4/\left(H_2C_2O_4\right)_0 = {} & 1/\left(\left(1/K_1K_2H^2\right)\right. \\ & \left. + \left(1/K_2H\right) + 1\right)\end{aligned} \tag{A14}$$

Only in this case, L′ is constant versus pH, since it is always equal to the initial concentration $(H_2C_2O_4)_0$.

Considering the absence of data for MH_iL_j complexes, it can be noted that for $pH > 3.8$, the major species formed are $C_2O_4^{2-}$. This means that, as a first approximation, $HC_2O_4^-$ can be neglected

for the metal complexes formation. On the other hand, if the oxalate ion gives a precipitate with the metal M^{n+}, a solubility product K'_{so} should exist:

$$K'_{so} = [M][L]^{(n/2)} \quad \text{(A15)}$$

L is $C_2O_4^{2-}$ in the Kratgen's symbolic formulae (in order to simplify the expressions, we will also use HL for $HC_2O_4^-$, and H_2L for $H_2C_2O_4$).

The same calculations that have been done for the metal ion (cf. Section 1.1) can also be repeated for the oxalate ions involved in the formation of the oxalate complexes, free or bounded to the metal.

If we are also in $M(OH)_n$ precipitation conditions, i.e. at a pH value where $[M]_0 > \Sigma p\ Mp(OH)_q$), then the concentration of M at the equilibrium is fixed by eqn (A5). The introduction of (A5) in (A15) gives the concentration of the oxalate:

$$[L] = (K'_{so}/(H^n \times *K_{so}))^{(2/n)} \quad \text{(A16)}$$

The different oxalate species in the solution can be estimated by substitution in (A10) and (A11), respectively:

$$HL = K_1 H^{(n-4)/n}\left(K'_{so}/*K_{so}\right)^{(2/n)} \quad \text{(A17)}$$

$$H_2L = K_1K_2H^{(2n-4)/n}\left(K'_{so}/*K_{so}\right)^{(2/n)} \quad \text{(A18)}$$

The species ML_a are defined by the cumulative stability constants:

$$\beta_a = [ML_a]/[M][L]^a \quad \text{(A19)}$$

and, by combination with (A15, A16), the concentration of oxalate complexes is given by

$$[ML_a] = \beta_a \times K'so \times [L]^{a-n/2} = \beta_a \times K'so^{2a/n}/(H \times *Kso^{1/n})^{(2a-n)} \quad \text{(A20)}$$

So, the mass balance for the oxalic acid, expressed as

$$[H_2L]_0 = H_2L + HL + L + ML + 2ML_2 + \ldots + n/2(ML_{n/2})_{prec.} \quad \text{(A21)}$$

can be directly solved, replacing the different species concentration by their respective solution of the reactions (A16)–(A20).

1.3 Out of dual precipitation conditions

If, at a pH value, the concentration of the introduced metal ion, $[M]_0$, does not reach the equilibrium conditions for precipitation of $M(OH)_n$, then eqn (A5) cannot be used. The mass balance for M [eqn (A1)] is then given by the following equation:

$$M_0 = M + M(OH) + \ldots + M(OH)_i + \ldots + pM_p(OH)_q + rM_r(L)_s + \ldots + (ML_{n/2})_{prec.} \quad \text{(A22)}$$

where $M(OH)_n$ prec. = 0 because no hydroxide precipitate is formed. Then, introducing the stability constants $*\beta_{qp}$, eqn (A22) becomes:

$$M_0 = M\left(1 + *\beta_1/H + \ldots + *\beta_{qp}M^{p-1}/H^q + \beta_{sr}\ M^{r-1}L^s + \ldots +\right) + (ML_{n/2})_{prec.} \quad \text{(A23)}$$

The mass balance for L must also be considered, using eqn (A21). M and Lare related by the solubility product, eqn (A15), since there is an oxalate precipitation. The M_0 and $[H_2L]_0$ are chosen considering the experimental concentrations.

Now, by substitution of L by M in eqn (A21), and reporting $(ML_{n/2})_{prec.}$ in eqn (A23), M can be found from a classical equation resolution method. For given M and pH values, the above calculations give the concentration for the different species.

The same kind of calculations can be done if only $[H_2L]_0$ is lower than the values needed to begin the precipitation, just modifying eqn (A21), and applying the same methodology as before. The resolution of this case is easier because M is directly given by $^*Kso$ [eqn (A5)] and then, the two mass balance equations, eqn (A21) (without precipitate) and eqn (A1) determine the hydroxide precipitation yield.

Out of precipitation equilibrium conditions, there also exists the case where, at a certain pH value, both $[M]_0$ and $[H_2L]_0$ are lower than the values for precipitation. This case has no practical interest, since no precipitate is formed.